

# LOSSLESS PROGRESSIVE TRANSMISSION OF SCIENTIFIC DATA USING BIORTHOGONAL WAVELET TRANSFORM

Hai Tao and Robert J. Moorhead

tao@erc.msstate.edu

rjm@erc.msstate.edu

NSF Engineering Research Center for Computational Field Simulation

P.O. Box 6176, Mississippi State University, Mississippi State, MS 39762

## ABSTRACT

A new progressive transmission scheme using spline biorthogonal wavelet bases is proposed in this paper. First, several wavelet bases are compared with the spline biorthogonal wavelet bases. By exploiting the properties of this set of wavelet bases, a fast algorithm involving only additions and subtractions is developed. Due to the multiresolutional nature of the wavelet transform, this scheme is compatible with hierarchical-structured rendering algorithms. The formula for reconstructing the functional values in a continuous volume space is given in a simple polynomial form. Lossless compression is possible, even when using floating-point numbers. When the algorithm is applied to data from a global ocean model, the lossless compression ratio is about 1.5:1. Even with a compression ratio of 50:1, the reconstructed data is still of good quality. Finally, the reconstructed data is rendered using various visualization algorithms and the results are demonstrated.

## 1. INTRODUCTION

Progressive transmission algorithms (Fig. 1) for scientific visualization have been previously proposed. E.g., Muraki [5] applied a truncated version of Battle-Lemarié wavelets to volume data and proposed a fast superposition algorithm for reconstructing function values in continuous space. However, there are still some unsolved problems. Most wavelet transform (WT) approaches slow down the system performance by introducing a time-consuming decoding procedure. This greatly limits their value in applications with strict speed requirements. In most visualization techniques, the function values in continuous space must be calculated conveniently. By using an infinitely supported function as the superposition basis, a complex approximation algorithm has to be utilized. Another drawback is that lossless data compression is difficult because the denominators of the coefficients often are not in the form of  $2^n$ .

In this paper, a scheme based on the spline biorthogonal wavelet transform (BWT) is proposed for progressive visualization of very large data sets. The lengths of all filters are less than 6. Because all the filter coefficients are dyadic rationals, multiplication and division operations can be simplified to additions and subtractions for floating-point numbers and to

shifts for integer numbers. This makes the transform much faster. This property also makes lossless coding possible. In the case of the BWT, symmetry is more easily achieved, resulting in a better handling of the data boundary. Because the transform basis functions are compactly supported and can be explicitly formulated in a polynomial form, the reconstruction of function values from WT coefficients is much easier.

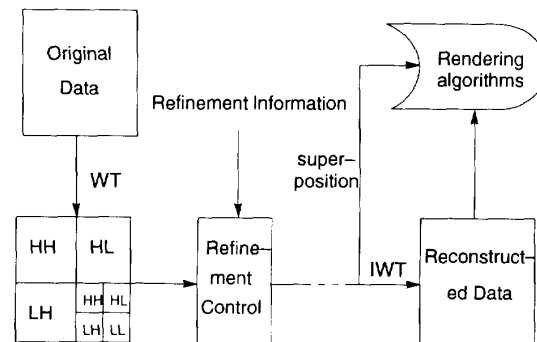


Figure 1: A block diagram of progressive transmission using a wavelet transform (WT).

## 2. METHOD

Basically, the scheme illustrated in Fig. 1 contains four steps: the WT and entropy coding, the entropy decoding and inverse WT, the refinement strategy, and the rendering algorithm. Since sophisticated methods for entropy coding and refinement control exist [2][3], the focus here is on the WT and the reconstruction of function values in continuous space.

### 2.1 Biorthogonal Wavelet Transform (BWT)

A simple WT decomposition and reconstruction scheme [4] using quadrature mirror filters (QMF) is shown in Fig. 2.  $g(n)$  is given by:

$$g_n = (-1)^n h_{-n+1} \quad (1)$$

There are many families of wavelet bases with reasonable decay both in the time and the frequency domain. However, to guarantee perfect reconstruction (PR), the filter can not be trun-

cated. This implies that the wavelet basis must be compactly supported. Also, to more easily deal with the data boundary, symmetric bases are preferred. It is well known from wavelet theory that symmetry and PR are incompatible if the transform in Fig. 2 is used. This difficulty can be overcome by using the BWT [1], which is diagrammed in Fig. 3.

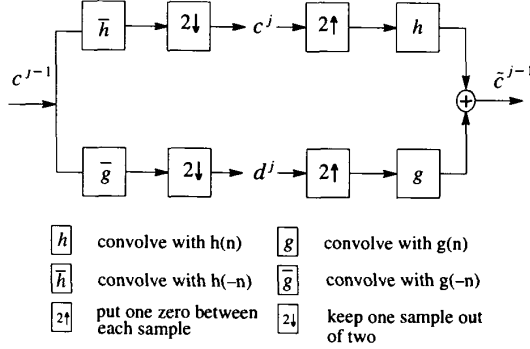


Figure 2: A block diagram of the basic wavelet decomposition and reconstruction scheme. Only one  $h$  is needed.

In this implementation,  $h$  and  $\tilde{h}$  are different but are both symmetric. Also,  $g$  and  $\tilde{g}$  satisfy:

$$\tilde{g}_n = (-1)^n h_{-n+1} \quad g_n = (-1)^n \tilde{h}_{-n+1} \quad (2)$$

If  $H(\xi)$  and  $\tilde{H}(\xi)$  are the Fourier-transforms of  $h$  and  $\tilde{h}$ , according to [1], a sufficient condition on  $H$  and  $\tilde{H}$  to make them PR filters is:

$$H(\xi)\tilde{H}(\xi) = \cos(\xi/2)^{2l} \cdot \left[ \sum_{p=0}^{l-1} \binom{l-1+p}{p} \sin(\xi/2)^{2p} + \sin(\xi/2)^{2l} R(\xi) \right] \quad (3)$$

where  $R(\xi)$  is an odd polynomial in  $\cos(\xi)$ , and  $2l = k + \tilde{k}$ , which means the length of  $h$  and  $\tilde{h}$  should be both even or both odd. If  $R \equiv 0$  and if  $\tilde{H}(\xi) = \cos(\xi/2)^k e^{jK\xi/2}$ , where  $K = 0$  if  $\tilde{k}$  is even and  $K = 1$  if  $\tilde{k}$  is odd,  $h$  and  $\tilde{h}$  are called spline filters since the related scaling function  $\tilde{\phi}$  is a B-spline function. Table I gives some example bases of this family.  $\tilde{H}(z)$  and  $H(z)$  are  $z$ -transforms of  $h$  and  $\tilde{h}$ . Notice that the denominators of the coefficients are all in the form  $2^n$ . This property makes them good candidates for the application. There is still some freedom left to choose bases from this family depending on implementation requirements. One basic principle is if a set of longer bases is used, the frequency separation property of  $h$  and  $g$  will be better, but the computational complexity will increase and the lossless compression ratio will decrease.

The visualization application involves rendering the data from numerous large (e.g., eighteen 75 MB) data files simultaneously. For efficient visualization, the inverse WT must be

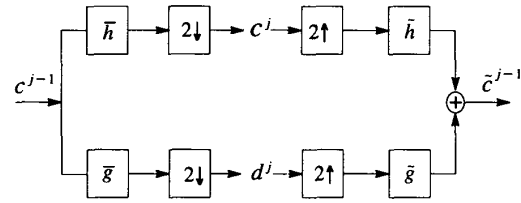


Figure 3: A block diagram of the biorthogonal wavelet decomposition and reconstruction scheme.  $h$  and  $\tilde{h}$  are different.

very fast. To accomplish this, a system using the wavelet bases in Table I with  $\tilde{k} = 2$  and  $k = 2$  has been implemented. Fig. 4 shows the scale function  $\tilde{\phi}(x)$  and the wavelet function  $\tilde{\psi}(x)$ .

$\tilde{k}$	$\tilde{H}(z)$	$k$	$H(z)$
1	$(1+z)$	1	$\frac{1}{2}(1+z)$
		3	$-\frac{z^{-2}}{16} + \frac{z^{-1}}{16} + \frac{1}{2} + \frac{z}{2} + \frac{z^2}{16} - \frac{z^3}{16}$
2	$\frac{1}{2}(z^{-1} + 2 + z)$	2	$-\frac{z^{-2}}{8} + \frac{z^{-1}}{4} + \frac{3}{4} + \frac{z}{4} - \frac{z^2}{8}$
		4	$\frac{3z^{-4}}{128} - \frac{3z^{-3}}{64} - \frac{z^{-2}}{8} + \frac{19z^{-1}}{64} + \frac{45}{64} + \frac{19z}{64} - \frac{z^2}{8} - \frac{3z^3}{64} + \frac{3z^4}{128}$

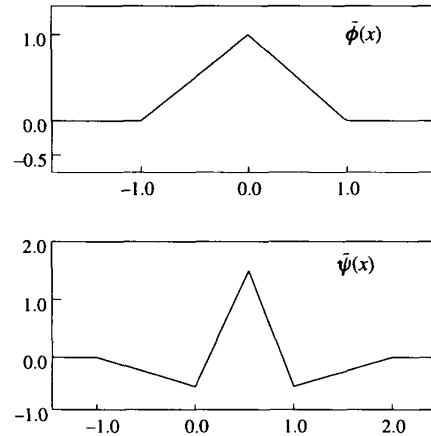


Figure 4: Scale function  $\tilde{\phi}(x)$  and wavelet function  $\tilde{\psi}(x)$  of the spline BWT in Table I when  $\tilde{k} = 2$  and  $k = 2$ .

## 2.2 Fast Wavelet Transform

The efficient WT method introduced by Mallat [4] borrowed the QMF scheme from subband coding theory (Fig. 2). In this algorithm, the major computational burden is caused by the convolution operation which involves floating-point multiplication. Because  $h$ ,  $\tilde{h}$ ,  $g$  and  $\tilde{g}$  are all symmetric in the proposed scheme, the number of multiplications is halved. For

numbers in IEEE standard floating-point format, multiplication by  $2^n$  can be simplified to the addition of  $n$  to the exponent, while for integers only a shift operation is needed.

### 2.3 Superposition

To combine a progressive transmission scheme with a visualization algorithm, the function values in the continuous volume must be approximated from the transform coefficients. In a general 1-D case, if the spline BWT with  $\bar{k} = 2$  and  $k = 2$  is used, the function value at  $x$  can be reconstructed using the following formula:

$$\hat{f}(x) = \sum_{j=-\infty}^{j=\infty} \bar{\phi}_{k,j}(x) + \sum_{j=-\infty}^{j=K} \tilde{\psi}_{i,j}(x)$$

where  $\bar{\phi}_{k,j}(x) = \sqrt{2^{-k}} \bar{\phi}(2^{-k} - j)$   
 $\tilde{\psi}_{i,j}(x) = \sqrt{2^{-i}} \tilde{\psi}(2^{-i} - j)$   
 $K = \text{levels of the WT}$  (4)

Since  $\bar{\phi}(x)$  is a set of compactly supported piecewise B-spline functions,  $\hat{f}(x)$  can be written in a closed polynomial form with order  $\bar{k} - 1$ . As shown in Fig. 4, the  $\bar{\phi}(x)$  and  $\tilde{\psi}(x)$  used herein are of order 1. The process of reconstructing the function values in continuous space from the WT coefficients is illustrated in Fig. 5. In each interval  $[i, i+1)$ , the reconstructed function is a linear function. Thus (4) can be simplified to:

$$\hat{f}(x) = (1 - q) \cdot \hat{f}(l) + q \cdot \hat{f}(l + 1)$$

where  $x \in [l, l + 1)$  and  $q = x - l$  (5)

This suggests that the exact function value at any real  $x$  can be computed through linear interpolation of the function values at the two discrete neighbors which surround  $x$ . In this case, the resulted  $\hat{f}(x)$  is  $C^0$  continuous. When the order of  $\bar{\phi}(x)$  and  $\tilde{\psi}(x)$  is larger than 1, formula (4) can still be written in a closed polynomial form with order of  $\bar{k} - 1$ .  $\hat{f}(x)$  will be  $C^{\bar{k}-2}$  continuous. If the tensor products of the one-dimension bases are used as the bases for the multidimension WT, the same conclusion can be drawn.

### 2.4 Implementation of Lossless Compression

IEEE single-precision floating-point numbers have 24 bits of precision. Multiplication by  $2^n$  will require no extra bits to retain the same precision. However, addition may result in some extra bits. As an example, consider the WT in the proposed scheme. For  $\bar{h}$ , the convolution formula is:

$$c_n = -\frac{1}{8} f_{n-2} + \frac{1}{4} f_{n-1} + \frac{3}{4} f_n + \frac{1}{4} f_{n+1} - \frac{1}{8} f_{n+2} \quad (6)$$

where  $f_i$  is the discrete input function value. Suppose the maximum and minimum exponents of all five  $f_i$  values are  $P_{max}$  and  $P_{min}$ , respectively. Then the maximum number of extra bits ( $\bar{b}_e$ )

needed to save  $c_n$  is  $P_{max} - P_{min} + 3$ . Similarly, for  $\tilde{h}$ , the maximum number of extra bits ( $\tilde{b}_e$ ) is  $P_{max} - P_{min} + 2$ . This is the worst case. Usually  $\bar{b}_e$  and  $\tilde{b}_e$  are less than the value given here. Recording the information about the extra bits using an oct-tree has worked well.

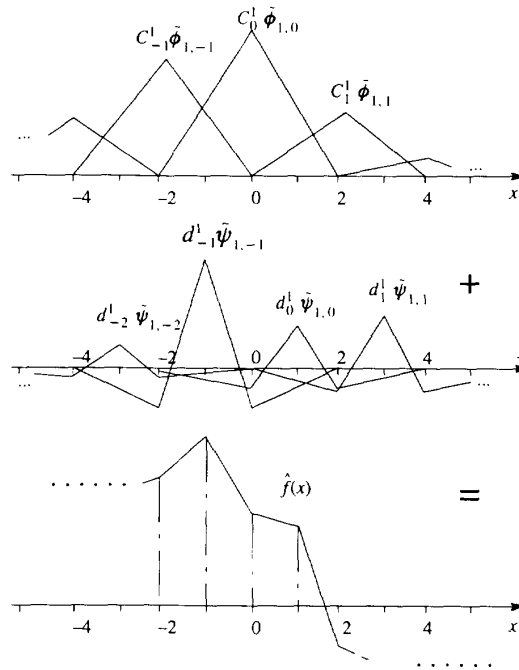


Figure 5: Reconstruction (superposition) of function values in continuous space using the spline BWT coefficients. Notice that  $\hat{f}(x)$  is a linear function in the interval  $[i, i+1)$ .

## 3. RESULTS

The scheme described in this paper was applied to time-varying ocean model data [6], sampled on a  $337 \times 468 \times 6$  grid 120 times per year. Layer thickness and current data in floating-point format — variables from the model — were visualized. Each of the six time-varying layers were considered separately.

The spline BWT was compared with a family of 6-tap WTs where all  $h_i$  are functions of two parameters —  $\alpha$  and  $\beta$  — according to the formulae in (7). Several 1-D signal sequences with 120 samples were arbitrarily chosen from the ocean model data set. For each test signal, the minimum MSE was found in the  $\alpha - \beta$  parameter space. Then it was compared with the MSE generated by the spline BWT compression algorithm. Table II gives the results. From these data, it was concluded that although the lengths of the spline BWT filters are less than 6, they perform the same or better than the optimized 6-tap WTs in a scheme where both forward and inverse transforms use the same filters.

$$\begin{aligned}
h_{-2} &= [(1 + \cos \alpha + \sin \alpha) \cdot (1 - \cos \beta - \sin \beta) + 2 \cos \beta \sin \alpha] / 4 \\
h_{-1} &= [(1 - \cos \alpha + \sin \alpha) \cdot (1 + \cos \beta - \sin \beta) - 2 \cos \beta \sin \alpha] / 4 \\
h_0 &= [1 + \cos(\alpha - \beta) + \sin(\alpha - \beta)] / 2 \\
h_1 &= [1 + \cos(\alpha - \beta) - \sin(\alpha - \beta)] / 2 \\
h_2 &= 1 - h_{-2} - h_0 \quad h_3 = 1 - h_{-1} - h_1 \\
\text{where} \quad & -\pi \leq \alpha, \beta \leq \pi
\end{aligned} \tag{7}$$

TABLE II

Test Signal 120 samples	6-Tap WT			Biorth. Spline WT $k = 2, k = 2, \text{MSE}$
	Optimal $\alpha$	Optimal $\beta$	MSE	
A	-1.0210	0.4712	0.0241	0.0143
B	1.4137	0.8639	0.0805	0.0537
C	1.4922	1.0210	0.0806	0.0513
D	-1.0210	0.3141	0.0099	0.0048
E	1.0995	0.3141	0.1521	0.0912
F	-1.4137	-0.8639	0.2364	0.0831
G	1.1780	0.4712	0.1947	0.0786

To apply the BWT to the data set, the boundary conditions had to be considered. In each frame (timestep) of ocean model data, valid function values are only available within the ocean area. This area was constant over time. A 2-D WT requires the ocean area to be approximated using  $2^n \times 2^n$  blocks, where  $n$  is larger than the level of the WT in each data frame. The approximated ocean area had to cover the entire original ocean area. For grid points in the approximated ocean area but not in the original area, second order Lagrange interpolation was used to yield function values. This introduced some discontinuity at the data boundary. Since all the WT bases are symmetric, the function values outside the boundary were achieved simply by reflection.

The WT scheme, shown in Figure 6, applies the transform twice in each spatial dimension in a frame and once in the temporal dimension. Even using only 1/32 of the transform coefficients, the reconstructed data met the requirements of the scientific visualization processes. By using the refinement control strategy proposed by Blandford [3], only a small amount of data is needed for a better reconstruction.

In Fig. 7, layer thickness data, which is compressed at the rate of 50:1 is visualized. For a 2-D vector field, the two components are encoded independently. Streamlines generated from both the original field and the field reconstructed using only 1/32 of the WT coefficients are shown in Fig. 8.

The decoding speed, an important factor in interactive visualization system, is about 10 frames/sec on an SGI Indigo<sup>2</sup> machine. This satisfies the need of fast volume rendering in the application.

#### 4. CONCLUSIONS AND FUTURE WORKS

A new scheme of progressive transmission using a spline BWT is proposed in this paper. This family of wavelet base functions is symmetric, compactly supported, and the QMF coefficients are dyadic rationals. These attractive features make this scheme advantageous in several aspects. The transform it-

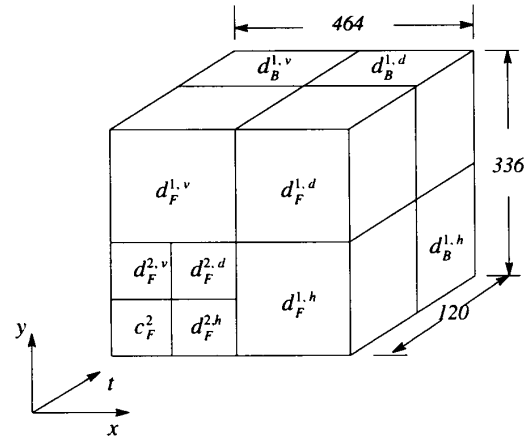


Figure 6: Wavelet transform coefficients of 3-D data of ocean model.

self is fast and high compression ratios can be achieved. The reconstructed data is of good quality and can be refined with a small amount of additional data. Data boundaries can be handled gracefully. The reconstruction of function values in continuous space from the WT coefficients utilizes a simple polynomial, which is especially useful for scientific visualization applications.

Future work includes more investigation of the WT's effects on the topology of the flow field, combining this algorithm with other hierarchical scientific visualization techniques, and constructing better wavelet bases.

#### 5. ACKNOWLEDGMENTS

This work has been supported in part by ARPA and the Strategic Environmental Research and Development Program (SERDP).

#### 6. REFERENCES

- [1] I. Daubechies, *Ten Lectures on Wavelets*, CBMS-NSF Regional Conference Series in Applied Mathematics, no. 61, Society for Industrial and Applied Mathematics, Philadelphia, PA, 1992.
- [2] Kou-Hu Tzou, "Progressive Image Transmission: A Review and Comparison of Techniques," *Optical Engineering*, 26(7), pp. 581-589, July 1987.
- [3] R. P. Blandford, "Wavelet Encoding and Variable Resolution Progressive Transmission," *NASA Space & Earth Science Data Compression Workshop Proceedings*, pp. 25-34, April 1993.
- [4] S. G. Mallat, "A theory for multiresolution signal decomposition: the wavelet representation," *IEEE Trans. Pattern Anal. Machine Intell.*, vol. 11, no. 7, July 1989.
- [5] S. Muraki, "Volume Data and Wavelet Transforms," *IEEE Computer Graphics & Applications*, pp. 50-56, July 1993.
- [6] H. E. Hurlburt, A. J. Wallcraft, Z. Sirkes, and E. J. Metzger, "Modeling of the Global and Pacific Oceans: On the Path to Eddy-Resolving Ocean Prediction," *Oceanography*, vol. 5, no. 1, pp. 9-18, 1992.



Figure 7a. Layer thickness for the NE Pacific Ocean – Original thickness data.



Figure 7b. Layer thickness for the NE Pacific Ocean – Reconstructed data (compression ratio = 50:1).

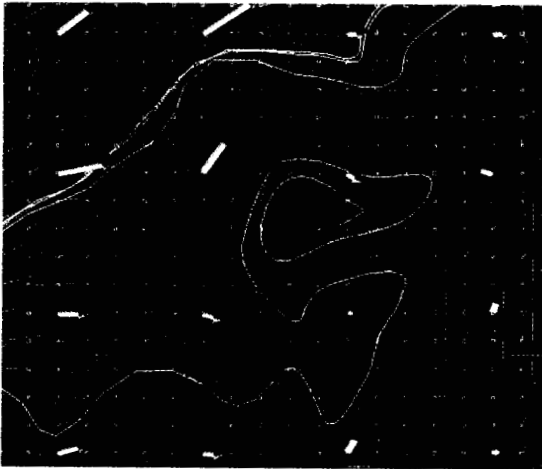


Figure 8a. Velocity data for the NE Pacific Ocean – Original data.

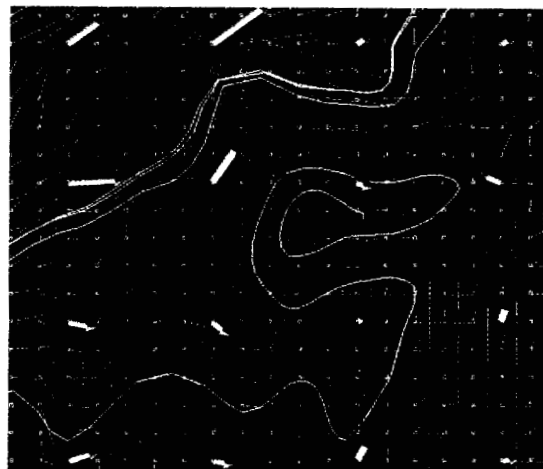


Figure 8b. Velocity data for the NE Pacific Ocean – Reconstructed data (compression ratio = 50:1).